August 15, 1993

P / 16

N94-14377

Coding Performance of the Probe–Orbiter–Earth Communication Link

D. Divsalar, S. Dolinar, and F. Pollara
Communications Systems Research Section

The coding performance of the Probe–Orbiter–Earth communication link is analyzed and compared for several cases. It is assumed that the coding system consists of a convolutional code at the Probe, a quantizer and another convolutional code at the Orbiter, and two cascaded Viterbi decoders or a combined decoder on the ground.

I. Introduction

Upon arrival at Jupiter on December 7, 1995, the Galileo spacecraft (herein referred to as the Orbiter) will relay data back to Earth from an atmospheric Probe released 5 months earlier. For about 75 min, data will be transmitted to the Orbiter from the Probe as it descends on a parachute to a pressure depth of 20–30 bars in the Jovian atmosphere. Shortly after the end of Probe relay, the Orbiter will ignite its rocket motor to insert into orbit about Jupiter. The orbital phase of the mission, referred to as the satellite tour, lasts nearly 2 years, during which time Galileo will complete 10 orbits about Jupiter [1].

The Probe–Orbiter–Earth communication link is illustrated in Fig. 1. The data sent from the Probe to the Orbiter are convolutionally encoded with the NASA standard (7,1/2) convolutional code. On board the Orbiter, receivers acquire, track, and package the Probe's data together with radio science and engineering data. The received encoded data are 3-bit quantized but not convolutionally decoded at the Orbiter.

Before the high-gain antenna anomaly occurred, the plan was to send Probe data packets over the Orbiter-to-Earth downlink in real time as the data were sent from the Probe to the Orbiter. Simultaneously, a backup copy of the received Probe data would be recorded via the Orbiter's tape recorder for later playback if needed. If Galileo is forced to use its low-gain antenna for the Orbiter-to-Earth downlink, real-time relay of the Probe's data is no longer possible, and the data playback from the tape recorder is now the primary rather than the backup system for returning the data to Earth.

The data to be played back from the tape recorder consist of 3-bit quantized convolutionally encoded symbols sent over the Probe-to-Orbiter link, and they are packaged together with other data in the Probe's data packet format. In particular, each 3-bit received symbol is padded with a zero fill bit in order to occupy a half-byte in the data packet.

As a backup to the tape recorder system, the Galileo Project now proposes to additionally record a reduced version of the Probe data in the Orbiter's computer memory to protect against catastrophic tape recorder failure. The data saved in this mode are 1-bit quantized received symbol data for a reduced portion of the Probe's total lifetime.

All Probe data sent from the Orbiter to Earth are to be convolutionally encoded with the same NASA standard (7,1/2) convolutional code. Additionally, the tape-recorded data are to be encoded with a (24,12) Golay outer code (as was the original real-time data). However, the data played back from computer memory will not be Golay encoded. On the ground, the plan is to perform all decoding operations independently, i.e., to first decode the Orbiter-to-Earth convolutional code, then the Golay code (if present), and finally the Probe-to-Orbiter code.

This article investigates the performance of such a communication link with 1-bit and 3-bit quantization at the Orbiter. Since the errors at the output of the inner Viterbi decoder come in bursts, the possibility of interleaving the data before the inner convolutional code to enhance the performance is also investigated. For the case of 1-bit quantization at the Orbiter, the possibility of using a single Viterbi decoder on the ground to decode the data encoded by the cascaded convolutional codes is also analyzed. The 3-bit quantization study is treated separately in Appendix B because it is based on a simplified model that does not strictly apply to the actual Galileo Probe coding system.

II. Simulation Study of Coding System "1-bit/Nominal"

The coding system block diagram for coding system "1-bit/Nominal" (nominal system with 1-bit quantization at the Orbiter) is shown in Fig. 2. Both convolutional codes have constraint length $K = 7$ and code rate $r = 1/2$. This case models the nominal backup system for the low-gain mission Probe–Orbiter–Earth link when the received symbols at the Probe are 1-bit quantized.

In this case, a hard limiter is used before the inner convolutional encoder. Let the information data rate at the outer convolutional code be R_{b1} bits per second. Denote the received power and the one-sided noise power spectral density at the input of a hard limiter by P_1 and N_{o1}, respectively. Then the received information bit signal-to-noise ratio $BSNR_1$ at the input of the hard limiter can be expressed as

$$BSNR_1 = \frac{E_{b1}}{N_{o1}} = \frac{P_1}{N_{o1}R_{b1}} \qquad (1)$$

Let the information data rate at the input of the inner convolutional code be R_{b2}. Let the received power and

one-sided power spectral density of the noise at the input of the inner Viterbi decoder be P_2 and N_{o2}, respectively. Then the received bit signal-to-noise ratio at the input of the inner Viterbi decoder can be written as

$$BSNR_2 = \frac{E_{b2}}{N_{o2}} = \frac{P_2}{N_{o2}R_{b2}} \qquad (2)$$

Note that for real-time operation $R_{b2} = 2R_{b1}$. However, the bits from the Probe are stored in the computer memory and therefore R_{b2} may not be related to R_{b1}. Simulation results for end-to-end bit error rate (BER) probability are shown in Figs. 3 and 4.

III. Simulation Study of Coding System "1-bit/Interleaved"

Bit errors at the output of Viterbi decoders occur in bursts. This implies that an outer decoder based on a conventional Viterbi algorithm is not optimal since it is not matched to the statistics of channels with memory. Therefore, the performance of coding system 1-bit/Nominal can be improved by using an interleaver before the inner convolutional code and a deinterleaver after the inner Viterbi decoder to randomize the bit errors at the output of the inner Viterbi decoder. The coding system of Fig. 2 with interleaving added to it is shown in Fig. 5. The end-to-end system bit-error probability is needed for this case (coding system "1-bit/Interleaved").

The channel between the output of the outer convolutional code and the output of the hard limiter can be modeled as a binary symmetric channel (BSC) with transition probability given by

$$\varepsilon_1 = Q\left(\sqrt{\frac{E_{b1}}{N_{o1}}}\right) \qquad (3)$$

where E_{b1}/N_{o1} represents the received bit signal-to-noise ratio at the input of the hard limiter.

The channel between the input of the ideal interleaver and the output of the deinterleaver can also be modeled as a memoryless BSC with transition probability ε_2. This channel consists of the inner convolutional code, the additive Gaussian noise channel, and the inner soft Viterbi decoder. The transition probability ε_2 and the overall bit error probability for the cascaded channel can be upper bounded analytically using transfer function bounding

techniques. This analysis is included in Appendix A. For comparison with coding system 1-bit/Nominal, more accurate actual bit-error rate curves are obtained by direct simulation. These simulation results are shown in Figs. 6 and 7.

IV. Simulation Study of Coding System "1-bit/Combined"

In order to improve the performance of the system in Fig. 3 at high $BSNR_1$, consider the modified system shown in Fig. 8.

In this system, the signal received at the ground station is decoded by a single Viterbi decoder which is designed for two cascaded rate 1/2, $K = 7$ convolutional codes with no noise between the encoders. The equivalent code for these two cascaded convolutional codes is a rate 1/4, $K = 10$ convolutional code that can be decoded with a 512-state decoder. The design of such a decoder requires knowledge of the generator polynomials of the equivalent code, denoted by $h_0(x)$, $h_1(x)$, $h_2(x)$, and $h_3(x)$. These polynomials can be found by the following method, which is a simplification and generalization of the method described in [4].

Consider the cascaded rate 1/2 convolutional codes shown in Fig. 9. In this figure

$$g_0(x) = 1 + x + x^2 + x^3 + x^6$$

$$g_1(x) = 1 + x^2 + x^3 + x^5 + x^6$$

and M represents a time multiplexing operation. One can obtain the generating polynomials of the equivalent code if one can move the middle multiplexer to the output. This can be done if one notes the equivalence between the two circuits shown in Fig. 10. In this figure, $f_e(x)$ and $f_o(x)$ represent the even and odd components of the polynomial $f(x)$. The values $f_e(x)$ and $f_o(x)$ are related to $f(x)$ as

$$f(x) = f_e(x^2) + x f_o(x^2)$$

Using this equivalence, one can move the middle multiplexer to the output and can obtain the circuit shown in Fig. 11, which is equivalent to the circuit in Fig. 9. In Fig. 11, $g_{0e}(x), g_{0o}(x)$ and $g_{1e}(x), g_{1o}(x)$ are the even and odd components of $g_0(x)$ and $g_1(x)$, respectively. This relation is defined as

$$g_0(x) = g_{0e}(x^2) + x g_{0o}(x^2)$$

$$g_1(x) = g_{1e}(x^2) + x g_{1o}(x^2)$$

where

$$g_{0e}(x) = 1 + x + x^3, \quad g_{0o}(x) = 1 + x$$

$$g_{1e}(x) = 1 + x + x^3, \quad g_{1o}(x) = x + x^2$$

Finally, using the equivalence between the two multiplexer circuits shown in Fig. 12, one obtains the structure of the equivalent code shown in Fig. 13. In this figure, $h_0(x)$, $h_1(x)$, $h_2(x)$, and $h_3(x)$ can be obtained as

$$h_0(x) = 1 + x + x^2 + x^6 + x^7 + x^8 + x^9$$

$$h_1(x) = 1 + x^2 + x^4 + x^5 + x^6$$

$$h_2(x) = x + x^2 + x^3 + x^8 + x^9$$

$$h_3(x) = 1 + x^2 + x^3 + x^4 + x^5 + x^6 + x^9$$

The system shown in Fig. 8 with a Viterbi decoder based on the polynomials $h_0(x)$, $h_1(x)$, $h_2(x)$, and $h_3(x)$ was simulated. The results of this simulation were compared to the performance of coding system 1-bit/Nominal, as shown in Fig. 14. As shown in this figure, there is more than a 3-dB gain in $BSNR_2$ for $BSNR_1 > 11$ dB.

V. Conclusion

Comparing the BER results for coding systems 1-bit/Nominal, 1-bit/Interleaved, and 1-bit/Combined, the authors conclude that interleaving improves the performance only for $BSNR_2 \leq 3$ dB. For the coding system 1-bit/Combined, there is a 3-dB improvement in $BSNR_2$ if $BSNR_1$ is larger than 11 dB.

These results may be directly applicable to predicting the end-to-end performance of Galileo's Probe data return for the case without the intervening Golay code. They may also be helpful in predicting performance of future missions that might also use cascaded convolutional codes such as Lander–Orbiter–Earth links.

References

[1] T. V. Johnson, C. M. Yeates, and R. Young, "Space Science Review Volume on Galileo Mission Overview," *Space Science Reviews*, vol. 60, no. 1-4, Kluwer Academic Publishers, pp. 3–21, 1992.

[2] E. Biglieri, D. Divsalar, P. McLane, and M. Simon, *Introduction to Trellis Coded Modulation with Applications*, New York: Macmillan, 1991.

[3] D. Forney, "Lower Bounds on Error Probability in the Presence of Large Intersymbol Interference," *IEEE Trans. on Communications*, vol. COM-20, pp. 76–78, February 1972.

[4] F. Pollara and D. Divsalar, "Cascaded Convolutional Codes," *The Telecommunications and Data Acquisition Progress Report 42-110*, vol. April–June 1992, Jet Propulsion Laboratory, Pasadena, California, pp. 202–207, August 15, 1992.
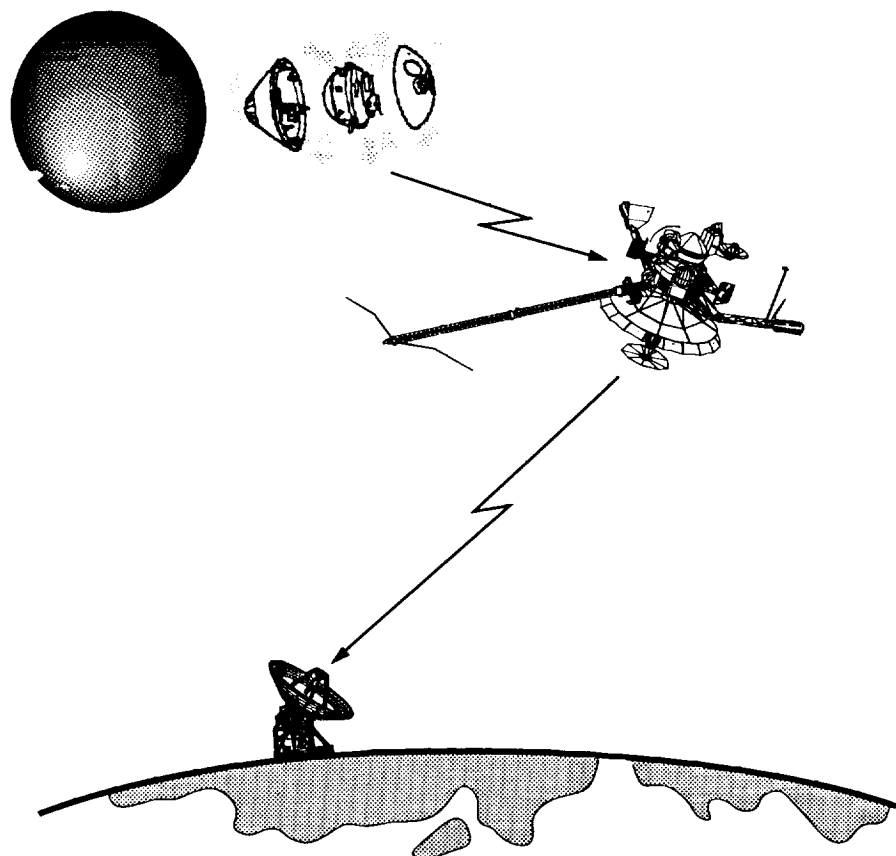
Fig. 1. Probe–Orbiter–Earth communication link.
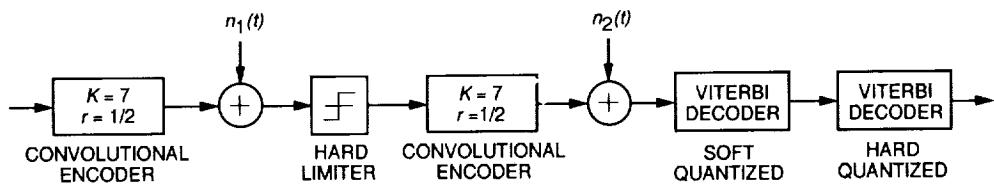
Fig. 2. Concatenated codes without interleaving: coding system 1-bit/Nominal.
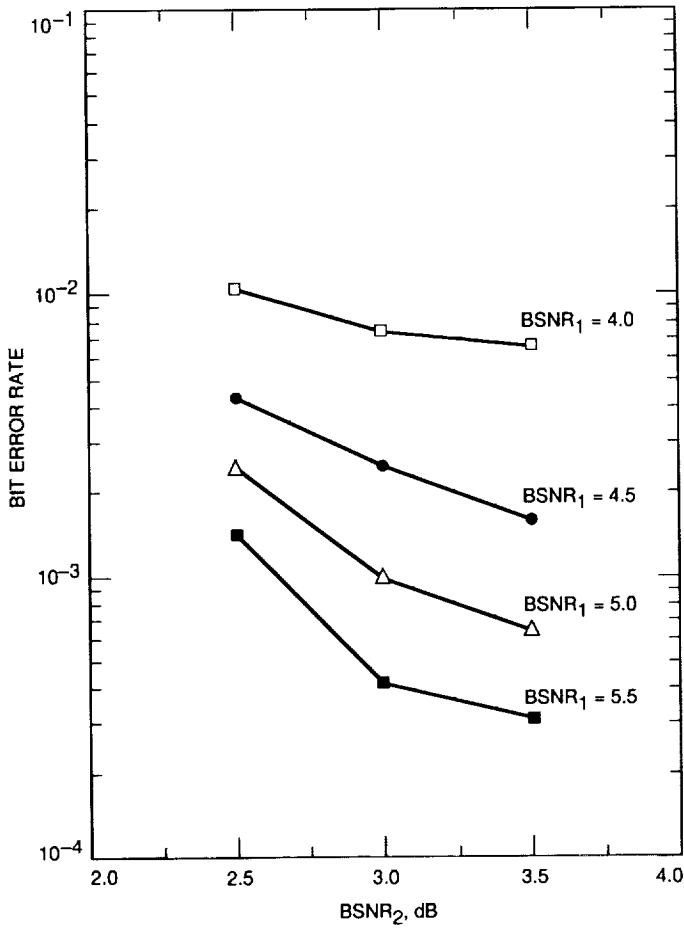
Fig. 3. BER simulation results for the coding system 1-bit/ Nominal (BER versus $BSNR_2$).
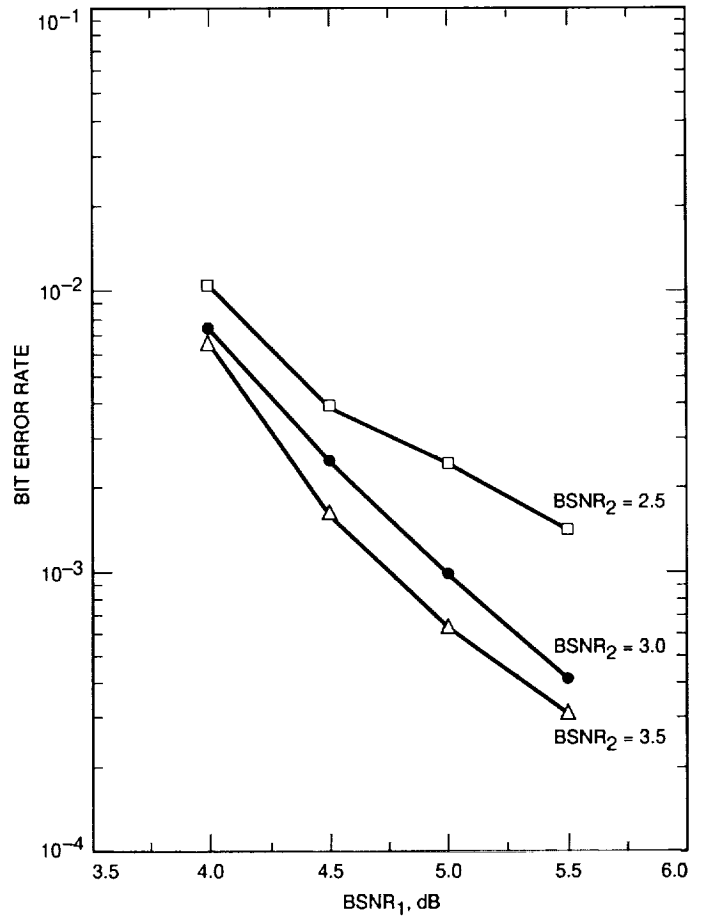
Fig. 4. BER simulation results for the coding system 1-bit/ Nominal (BER versus $BSNR_1$).
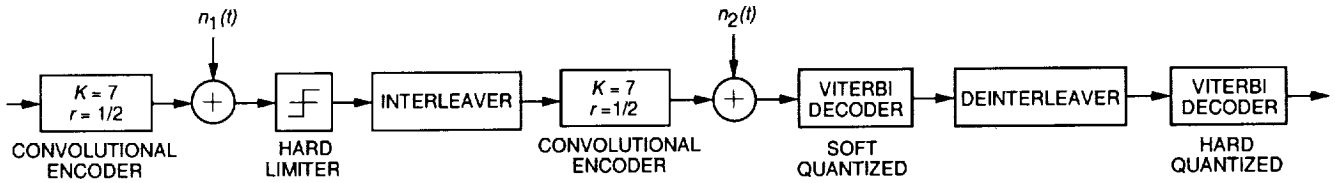
Fig. 5. The coding system 1-bit/Interleaved.
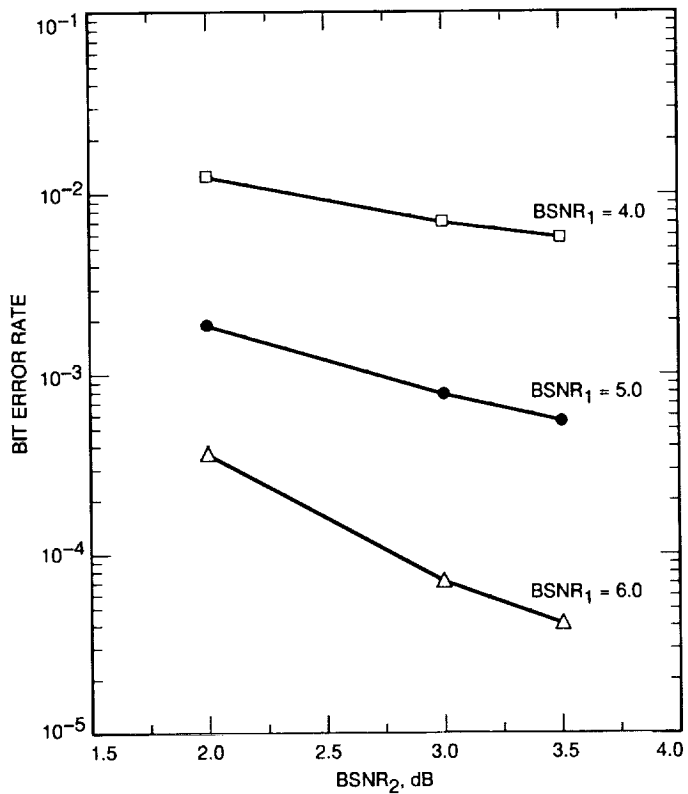
Fig. 6. BER simulation results for the coding system 1-bit/
interleaved (BER versus $BSNR_2$).
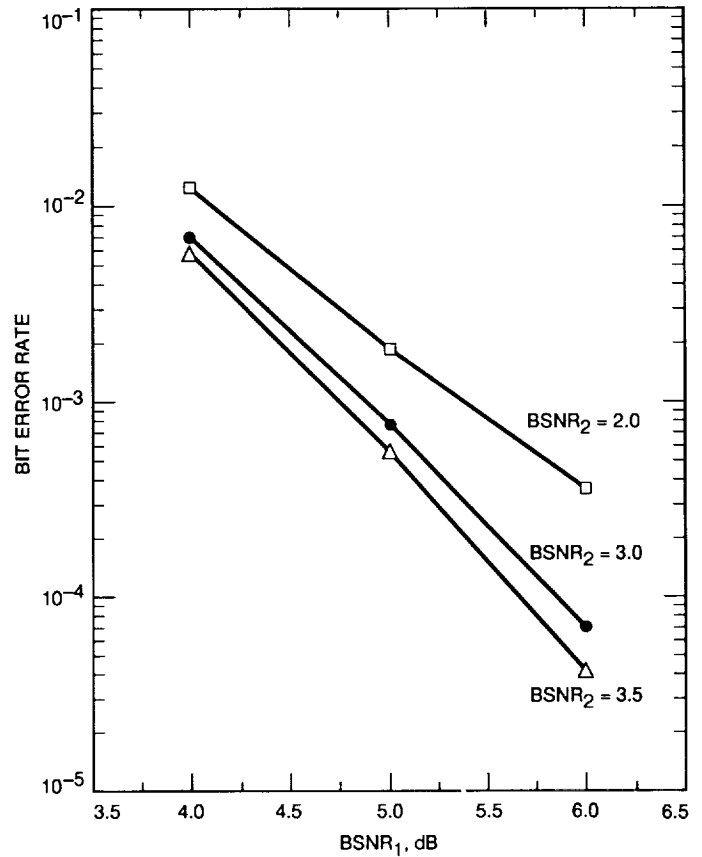
Fig. 7. BER simulation results for the coding system 1-bit/
interleaved (BER versus $BSNR_1$).
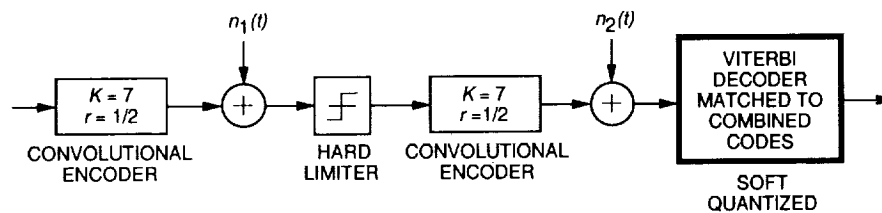
Fig. 8. The coding system 1-bit/Combined.
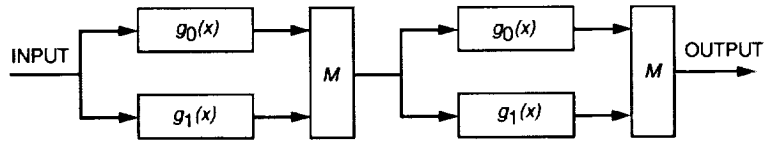
Fig. 9. Cascaded convolutional codes.
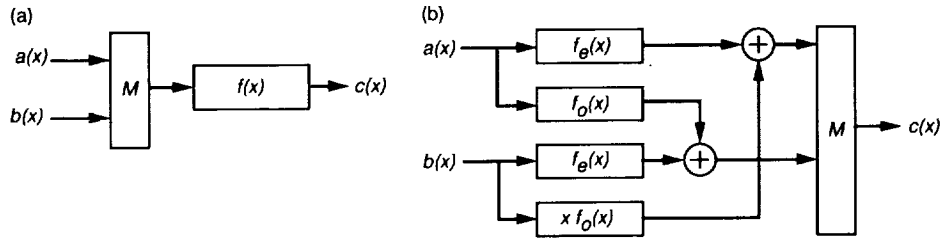
Fig. 10. Equivalent circuits: circuit (a) is equivalent
to circuit (b).
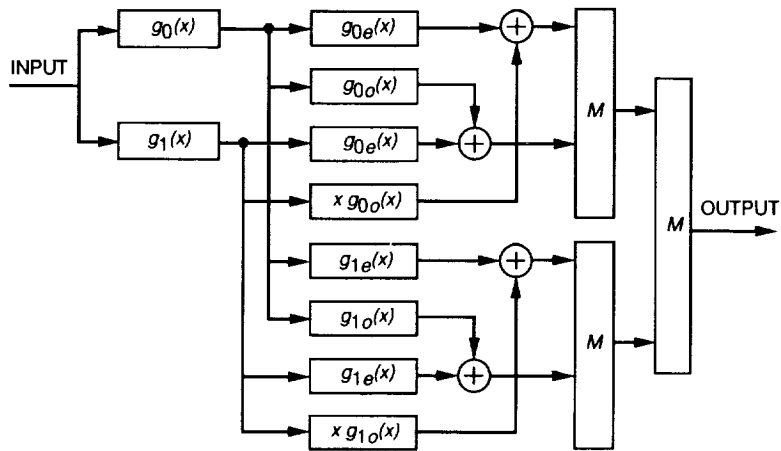
Fig. 11. Equivalent code.
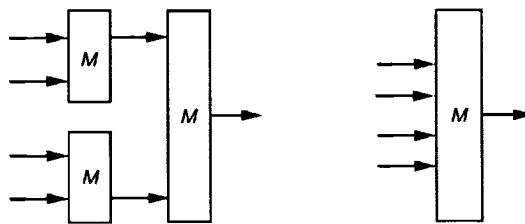
Fig. 12. Equivalent multiplexers.

75

$$h_0(x) = g_0(x)\, g_{0e}(x) + x\, g_1(x)\, g_{0o}(x)$$

$$h_1(x) = g_0(x)\, g_{1e}(x) + x\, g_1(x)\, g_{1o}(x)$$

$$h_2(x) = g_0(x)\, g_{0o}(x) + g_1(x)\, g_{0e}(x)$$

$$h_3(x) = g_0(x)\, g_{1o}(x) + g_1(x)\, g_{1e}(x)$$
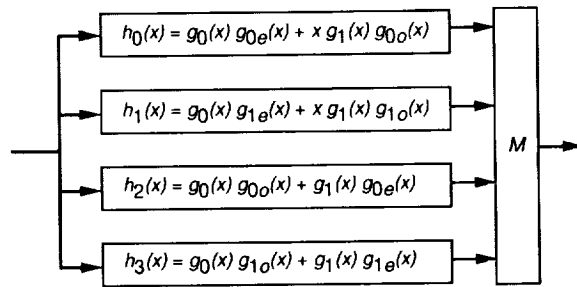
Fig. 13. Simplified equivalent code.
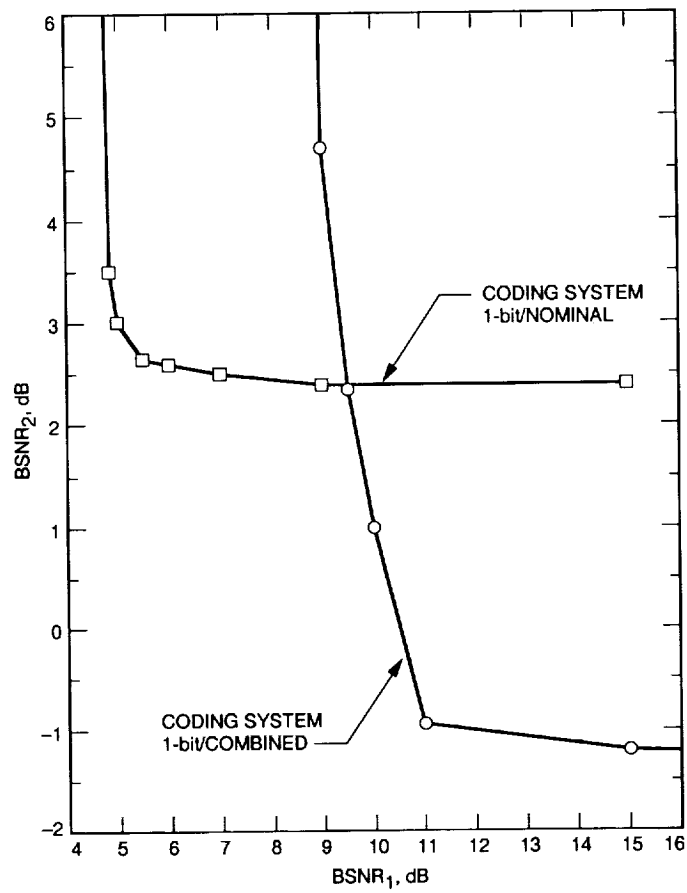
Fig. 14. Simulation comparison of the coding system 1-bit/
Nominal and the coding system 1-bit/Combined for BER = 10^{-3}.

Appendix A

Transfer Function Bounds for Coding System "1-bit/Interleaved"

The transition probability ε_2 can be computed using the transfer function bound on the bit error probability of the inner channel as [2]

$$\varepsilon_2 \leq Q\left(\sqrt{10\frac{E_{b2}}{N_{o2}}}\right) e^{\frac{5E_{b2}}{N_{o2}}} \frac{\partial}{\partial I} T(D_2, I)|_{I=1} \qquad (A\text{-}1)$$

where E_{b2}/N_{o2} represents the received bit signal-to-noise ratio at the input of the inner Viterbi decoder and D_2 is given by

$$D_2 = e^{-\frac{E_{b2}}{2N_{o2}}} \qquad (A\text{-}2)$$

The coefficients β_d of the transfer function bound

$$\frac{\partial}{\partial I} T(D_2, I)|_{I=1} = \sum_{d=d_f}^{\infty} \beta_d D^d \qquad (A\text{-}3)$$

(truncated to 15 terms) for the $K = 7$, $r = 1/2$ convolutional code with free distance $d_f = 10$ are given in Fig. A-1.

A tighter upper bound for the transition probability ε_2 can be obtained as [2]

$$\varepsilon_2 \leq \sum_{d=d_f}^{\infty} \beta_d Q\left(\sqrt{\frac{dE_{b2}}{N_{o2}}}\right) \qquad (A\text{-}4)$$

where d's and β_d's are given in Fig. A-1. The two cascaded BSC's, with transition probabilities ε_1 and ε_2, can be modeled as a single BSC with transition probability ε, which is related to ε_1 and ε_2 as

$$\varepsilon = \varepsilon_1 + \varepsilon_2 - 2\varepsilon_1\varepsilon_2 \qquad (A\text{-}5)$$

The cascaded channels and the equivalent BSC are shown in Fig. A-2.

Now it can be assumed that the outer convolutional code and its Viterbi decoder are operating over this single BSC with transition probability ε. An upper bound

for the end-to-end system bit error probability P_b can be obtained once again by using the transfer function bound and Fig. A-1. Then the transfer function bound on P_b can be expressed as [2]

$$P_b \leq \frac{1}{2} \sum_{d=d_f}^{\infty} \beta_d D_1^d \qquad (A\text{-}6)$$

where

$$D_1 = \sqrt{4\varepsilon(1-\varepsilon)} \qquad (A\text{-}7)$$

The upper bound on the end-to-end bit error probability versus $\text{BSNR}_1 = E_{b1}/N_{o1}$ and $\text{BSNR}_2 = E_{b2}/N_{o2}$ is shown in Figs. A-3 and A-4. The required BSNR_1 and BSNR_2 to achieve bit error probability of 10^{-3} using the upper bound in Eq. (A-6) is shown in Fig. A-5.

A simple lower bound on the bit error probability can be obtained by using an argument discussed in [3] that is based on a "genie" providing side information to the decoder. The performance of such a genie-aided decoder will be better than that of an actual decoder. Thus, this argument provides a lower bound on the performance of an actual decoder. For linear convolutional codes, the genie observes the transmitted sequence $\mathbf{x}$ and then reports to the receiver that the transmitted sequence was either $\mathbf{x}$ or a sequence $\hat{\mathbf{x}}$ within the distance d_f (the free distance of the code) from $\mathbf{x}$. Then a lower bound on the bit error probability of rate $1/n$ codes can be obtained as

$$P_b \geq P_{d_f} \qquad (A\text{-}8)$$

where P_{d_f} represents the pair-wise error probability between $\mathbf{x}$ and $\hat{\mathbf{x}}$, separated by d_f. For this case then the lower bound on ε_2 is

$$\varepsilon_2 \geq Q\left(\sqrt{\frac{dE_{b2}}{N_{o2}}}\right) \qquad (A\text{-}9)$$

Finally, for even d_f one can obtain a lower bound on the end-to-end bit error probability as

$$P_b \geq \sum_{k=d_f/2+1}^{d_f} \binom{d_f}{k} \varepsilon^k (1-\varepsilon)^{d_f-k}$$

$$+ \frac{1}{2} \binom{d_f}{d_f/2} \varepsilon^{d_f/2}(1-\varepsilon)^{d_f/2} \qquad \text{(A-10)}$$

where $d_f = 10$ and ε is given by Eq. (A-5) with ε_2 replaced by the lower bound in Eq. (A-9). Unfortunately, the lower bound on the bit error probability is not tight. For high signal-to-noise ratios, the lower bound is 1/36th of the upper bound. For this reason, simulation results are also provided for this case, as shown earlier in Figs. 6 and 7.

C-2

d	β_d
10	36
11	0
12	211
13	0
14	1404
15	0
16	11633
17	0
18	77433
19	0
20	502690
21	0
22	3322763
23	0
24	21292910

Fig. A-1. Transfer function bound coefficients
for the $K = 7, r = 1/2$ convolutional code.
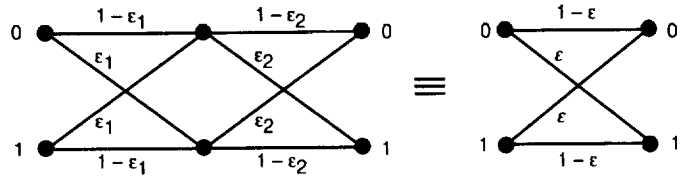
Fig. A-2. Cascaded BSC channels.
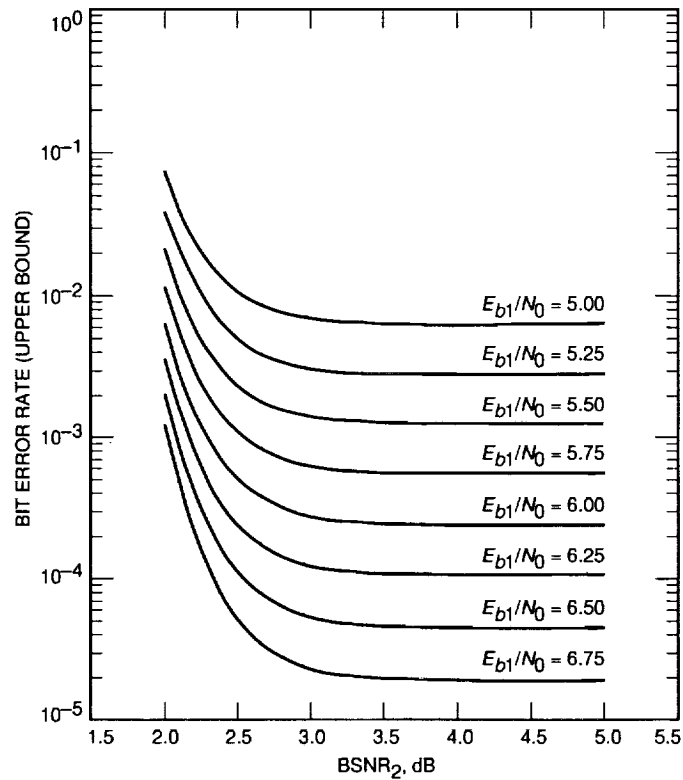
Fig. A-3. BER performance analysis for the coding system 1-bit/
interleaved (BER upper bound versus BSNR$_2$).
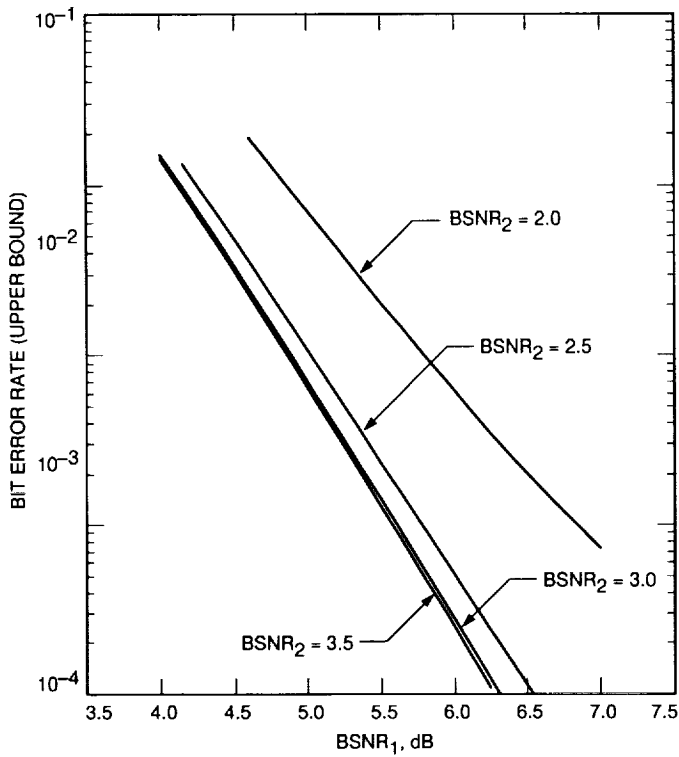
Fig. A-4. BER performance analysis for the coding system 1-bit/
interleaved (BER upper bound versus $BSNR_1$).
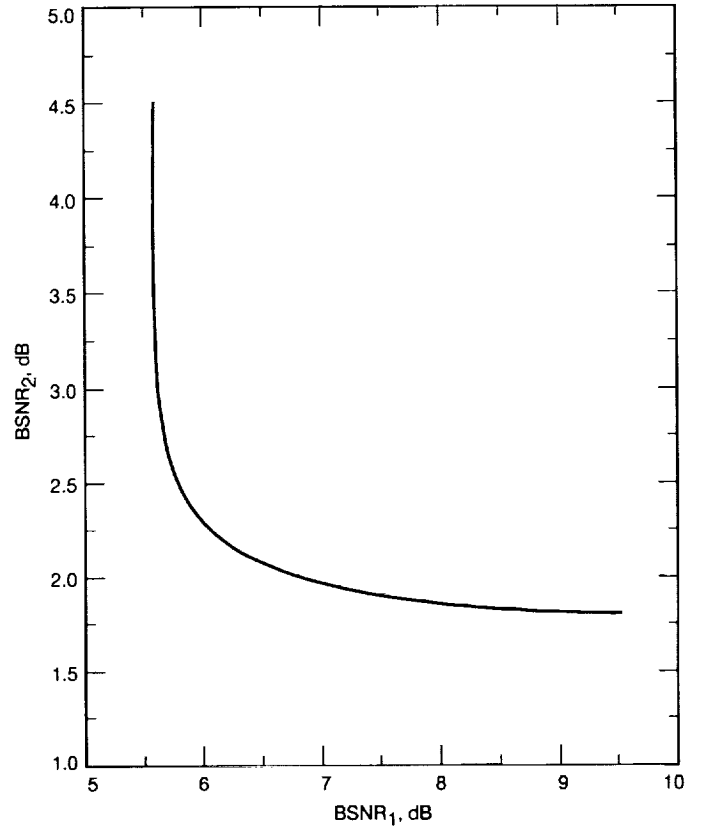
Fig. A-5. Required $BSNR_1$ and $BSNR_2$ to achieve BER = 10^{-3}
(upper bound).

Appendix B

Simulation Studies of 3-bit Quantized Coding Systems

In this appendix, two different analogues of the coding system 1-bit/Nominal are analyzed for the case of 3-bit quantization at the Orbiter. Neither one of these cases models the actual Galileo Probe coding system using 3-bit symbols stored in the Orbiter tape recorder, because the effects of the Golay code are not included in this analysis.

I. Simulation Study of Coding System 3-bit/No-Fill

The block diagram for coding system "3-bit/No-Fill," which includes separate decoders and 3-bit quantization at the Orbiter, is shown in Fig. B-1.

In this case, a 3-bit quantizer is used before the inner convolutional code. The received information bit signal-to-noise ratio at the input of the quantizer is given by Eq. (1). The received information bit signal-to-noise ratio for the inner convolutional code is given by Eq. (2).

Simulation results for end-to-end bit error probability are shown in Figs. B-2 and B-3.

II. Simulation Study of Coding System 3-bit/Fill

The block diagram for coding system "3-bit/Fill," which includes 3-bit quantization and an added fill bit at the Orbiter, is shown in Fig. B-4.

In this case again, a 3-bit quantizer is used before the inner convolutional code. But now for every 3 bits out of the quantizer, a "0" fill bit is inserted. The received information bit signal-to-noise ratio at the input of quantizer is given by Eq. (1). The received information bit signal-to-noise ratio for the inner convolutional code is given by Eq. (2).

Since the inserted 0's are known at the inner Viterbi decoder, one can use a known-state forcing algorithm to enhance the performance. The known-state forcing algorithm simply adds a vector $(N, 0, N, 0, \ldots)$ to the state metric vector, periodically, at the times corresponding to zero bit fills. The value N can be chosen appropriately to prevent buffer overflow. No zero component of this vector corresponds to states having a zero in the least significant place. Simulation results for end-to-end bit error probability are shown in Figs. B-5 and B-6.

Comparing coding systems 3-bit/No-Fill and 3-bit/Fill, there is a loss of about $10 \log_{10} 4/3 \approx 1.25$ dB for the coding system 3-bit/Fill due to the change of transmission rate, but there is a gain of about 1 dB by using known state forcing. Therefore, it seems that the overall performances of coding systems 3-bit/No-Fill and 3-bit/Fill are very close to each other. Comparing coding system 3-bit/No-Fill with coding system 1-bit/Nominal, one concludes that coding system 3-bit/No-Fill offers about 2 dB of performance improvement.
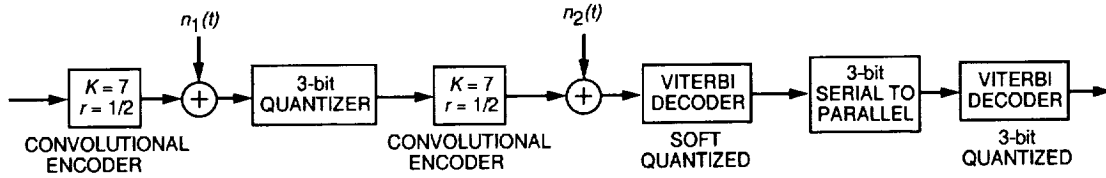
Fig. B-1. Block diagram for the coding system 3-bit/No-fill.
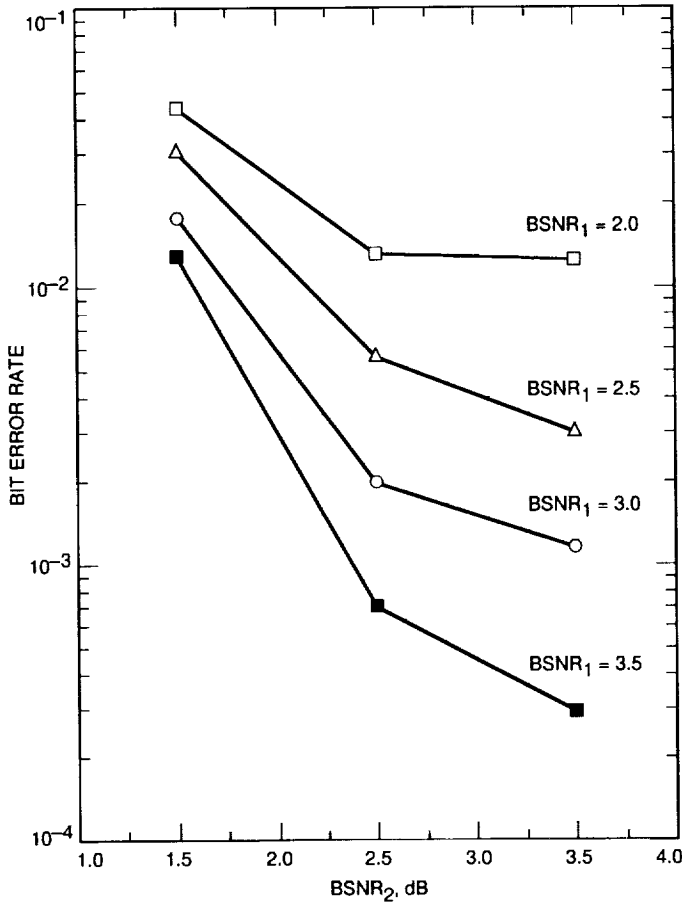
Fig. B-2. BER simulation results for the coding system 3-bit/No-fill (BER versus $BSNR_2$).
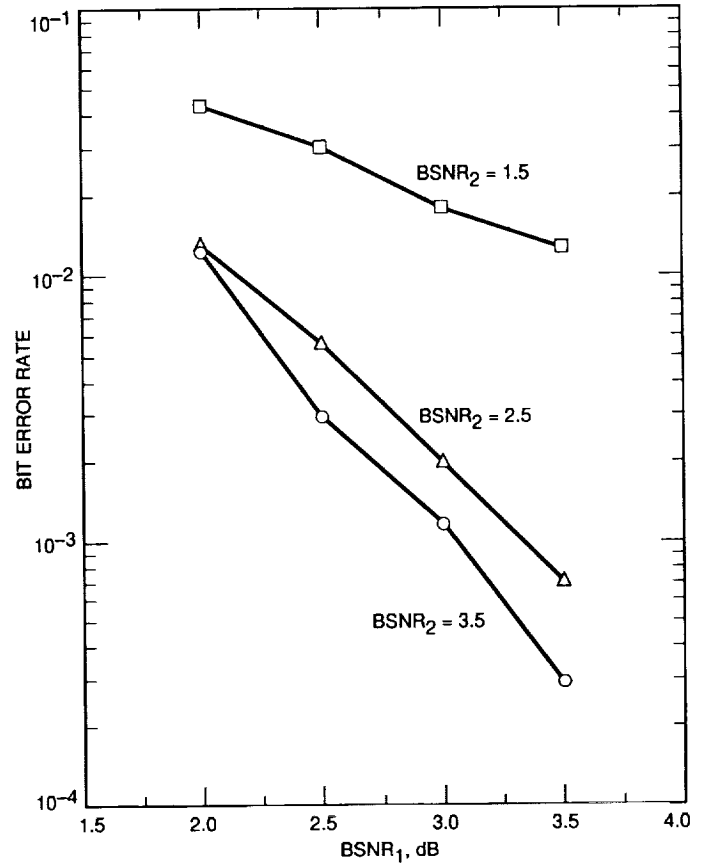
Fig. B-3. BER simulation results for the coding system 3-bit/No-fill (BER versus $BSNR_1$).
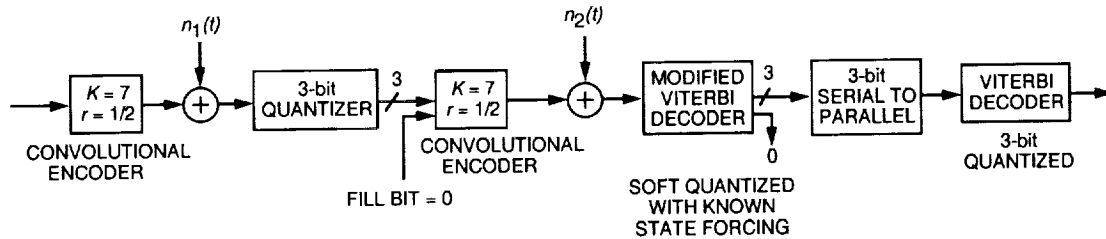
Fig. B-4. Block diagram for the coding system 3-bit/Fill.
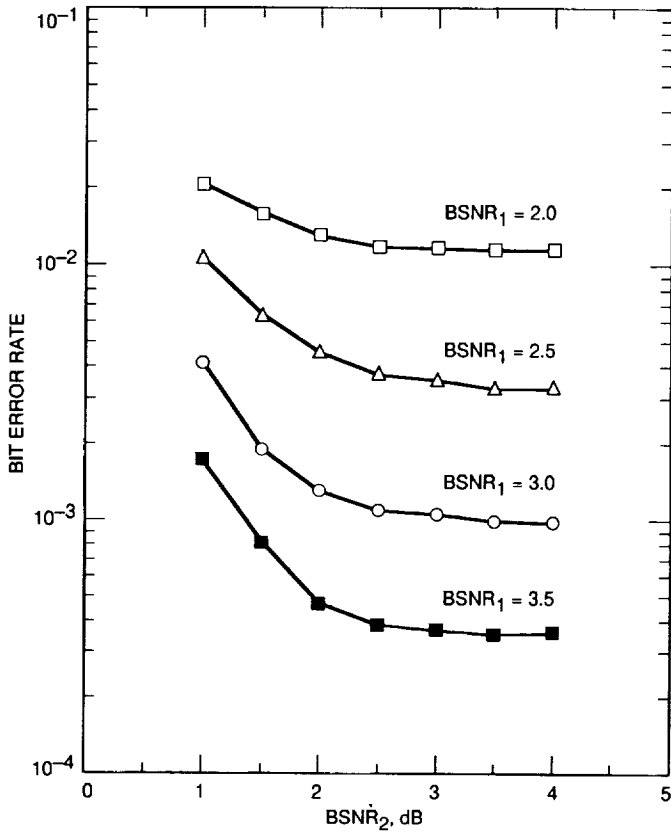
Fig. B-5. BER simulation results for the coding system
3-bit/Fill (BER versus $BSNR_2$).

Fig. B-6. BER simulation results for the coding system
3-bit/Fill (BER versus $BSNR_1$).